Surface Charge

Gerald Ehrenstein

Outline

I Introduction
II Gouy-Chapman Theory
III Experimental Evidence Supporting Gouy-Chapman Theory
IV Experimental Evidence Disagreeing with Gouy-Chapman Theory
V Possible Resolution of Experimental Differences
VI Significance of Surface Charge

I Introduction

The overall magnitude of the electric charge on a cell can be determined by measurement of the cell's electrophoretic mobility. Such a measurement provides an estimate of the average charge density over the entire cell membrane. This chapter will be concerned not with this average surface charge density, but rather with the local surface charge density in and near voltage-dependent ionic channels. The primary method of measuring local charge density is to examine the electrical properties of the voltage-dependent channels under normal conditions and under conditions where the surface charge near the channel is neutralized, thus changing the local electric field. Since voltage-dependent channels are sensitive to this local electric field, neutralization of surface charge is expected to cause changes in voltage-dependent properties, such as conductance and time constants. If surface charge were static, it would be expected that a particular neutralization of surface charge would cause a corresponding change in electric field, leading to a translation of all voltage-dependent properties along the voltage axis. The magnitude of the charge neutralization can be determined by measurement of the magnitude of the translation.

II Gouy-Chapman Theory

Gouy-Chapman theory describes the effect of a static surface charge on the membrane potential. A negative surface charge leads to formation of a double layer, since positive ions in solution tend to balance the negative surface charge. For simplicity, we will only consider external surface charge. This is the relevant case for most experiments, where ion substitutions are only made in the external solution.

Before considering the mathematical description of the electrical potential of the double layer, we consider a qualitative physical description. In the absence of surface charge, the resting potential across the membrane depends on the concentration and membrane permeability of the several ions. When external negative surface charge is added, a double layer is formed, and the electric field in this double layer results in a potential difference across it. The electric field in the external double layer is generally in the same direction as the electric field in the membrane. The overall potential difference does not change, since it must still balance the effect of the concentration and membrane permeability of the several ions. Therefore, the addition of a negative surface charge causes a decrease in the magnitude of the potential difference across the membrane proper. The usual method for obtaining information about the surface charge is to neutralize it, at least partially, by the addition of polyvalent cations, and to measure voltage-dependent properties for different amounts of neutralization. The neutralization of the negative surface charge may be caused by binding, by screening, or by both.

Under the assumptions that the external surface charge is uniformly distributed and that the membrane is homogeneous, the expression relating the double-layer potential, the external surface charge density, and the ionic concentrations in the external solution is (Grahame, 1947; Gilbert and

(1) $$\sigma_t = \frac{1}{G}\left\{ \sum_{i=1}^{n} C_i\left(\exp\left(-Z_i FV / RT\right) - 1\right)\right\}^{1/2}$$

Ehrenstein, 1969):

where σ_t = negative surface charge density per unit area in the absence of neutralization
G = constant at a given temperature
n = number of ionic species
C_i = concentration in the external solution of ion i
Z_i = valence of ion i
F = Faraday constant
V = potential across the double layer
R = gas constant
T = temperature

If σ_t is expressed in units of electronic charges per square nanometer,

(2) $G = 2.7$ (nm^2/electronic charge) $(moles/liter)^{1/2}$

Equation (1) applies when there is no binding to the surface charges. Many experiments have used the addition of polyvalent cations to the external solution to neutralize surface charges, and thus to probe their properties. When additional polyvalent cations are added to the external solution, the equilibrium constant k for cation binding is:

(3) $k = (MS)/M_mS$

where MS = neutralized site concentration
M_m = polyvalent cation concentration at the membrane
S = free negative surface charge concentration

The relation between M_m, the polyvalent cation concentration at the membrane, and M, the polyvalent cation concentration in the external solution, is the Boltzmann factor:

(4) $M_m = M \exp(-Z_M FV/RT)$

where Z_M = valence of polyvalent cation

We assume that each surface charge is either free or completely neutralized. This is equivalent to assuming that the valence of the polyvalent cations and the valence of the negative surface charge are equal. Then, S_t, the total negative surface charge concentration in the absence of neutralization, is:

(5) $S_t = S + MS$

Combining Equations (3) and (5),

(6) $S/S_t = 1/(1 + kM_m)$

In the above treatment, S is the negative surface charge concentration per unit volume. If we define σ as the negative surface charge concentration per unit area, σ and S are proportional, and an equation can be written for σ and σ_t that is similar to Equation (6) for S and S_t :

(7) $\sigma/\sigma_t = 1/(1 + kM_m)$

Combining Equations 1, 4, and 7, we find a general expression for the charge density:

(8) $$\sigma = \frac{1}{G\left(1 + kM\exp\left(-Z_M FV / RT\right)\right)}\left[\sum_{i=1}^{n} C_i\left(\exp\left(-Z_i FV / RT\right) - 1\right)\right]^{1/2}$$

Equation (8) relates the effective surface charge density σ to the membrane potential V and to the concentration of a neutralizing cation. This concentration appears in 2 places: the term M, which relates to binding, and one of the C_i, which relates to screening.

III Experimental Evidence Supporting Gouy-Chapman Theory

A common experimental approach to the measurement of local surface charge is to determine the values of a voltage-dependent property of an ion channel as a function of applied voltage for a range of divalent ion concentrations. According to Equation (8), for a given divalent ion concentration, there is a unique value for the effective surface charge and hence a unique value for the voltage of the double-layer Therefore, according to Gouy-Chapman theory, for any curve describing a voltage-dependent property as a function of voltage, a change in divalent ion concentration should shift the curve along the voltage axis by an amount equal to the voltage of the

double-layer, with no change in the shape of the curve. The theory further predicts that for a given channel and for a given divalent ion concentration, the voltage shifts will be the same for all voltage-dependent parameters - those related to the gating current as well as those related to the ionic current.

There have been a number of experimental confirmations of these predictions for a variety of channels. A good example is work on the sodium channel of frog skeletal muscle fibers (Hahin and Campbell, 1983). As shown in Fig. 1, high calcium concentration causes equal shifts in the kinetics of both ionic and gating currents.

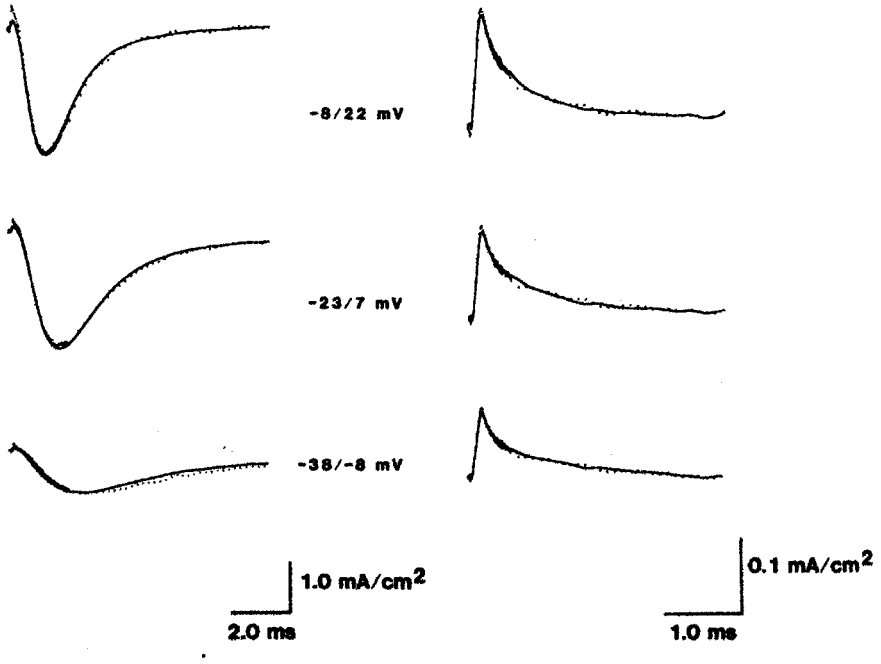

Figure 1. High Ca causes equal shifts in the kinetics of both ionic and gating currents. Superimposed on traces recorded in 2 mM Ca (solid traces) are traces recorded in 40 mM Ca at potentials 30 mV more positive (dots). Left: Na currents. The current calibration is for the currents recorded in 2 mM Ca. The currents recorded in 40 mM Ca have been scaled so that the peaks approximately coincide with the control current traces in order that the time courses may be compared. From top to bottom, the calibration bar represents 0.26, 0.46, and 0.33 mA/cm^2 for the 40 mM Ca traces. Right: gating currents recorded in 2 and 40 mM Ca at the same potentials as the ionic currents at the left. Both sets of gating current records are displayed at the same gain. Muscle 93, temperature 5°C, holding potential –150 mV. (From Hahin, and Cambell, 1983)

A more complete description of the shifts for some of the parameters is shown in Figs. 2, 3, and 4, and a summary of all the voltage shifts is shown in Table I. For an increase in calcium concentration from 2 mM to 40 mM, Table I indicates that all 6 parameters listed have voltage shifts of about 31 mV in the depolarizing direction.

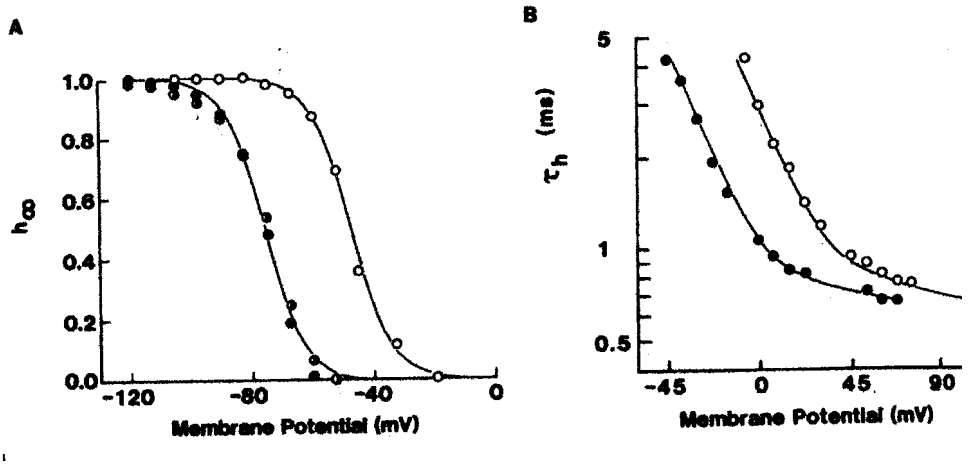

Figure 2: High Ca shifts the voltage dependence of inactivation. (A) Steady state inactivation in 2 and 40 mM Ca determined with a two-pulse protocol. The relative amplitude of the peak Na current elicited by test pulses to 0 mV is plotted against the variable potential during the 100-ms conditioning pulses. The peak currents were normalized relative to the maximum current obtained for the 0-mV test pulse in each solution. Control values were measured in 2 mM Ca before (filled circles) and after (half-filled circles) exposure to 40 mM Ca (open circles). The two curves wsere computed according to the function:

$$h_\infty = 1/(1 + \exp[(\boldsymbol{E} - \boldsymbol{E}_n)/k]$$

with identical slope factors k of 6.4 mV, midpoints E_h of –75 mV (control), and –46 mV (40 mM Ca). (B) τ_h vs. voltage. Shown are time constants determined from fits of single exponentials to the falling phase of Na ionic currents at 2 (filled circles) and 40 mM Ca (open circles). The curve through the 2 mM Ca points was drawn by eye, and the identical curve shifted 31 mV in the depolarizing direction is shown superimposed on the 40 mM Ca points. Fiber 72, temperature 6° C, holding potential –150 mV. (From Hahin and Cambell, 1983)

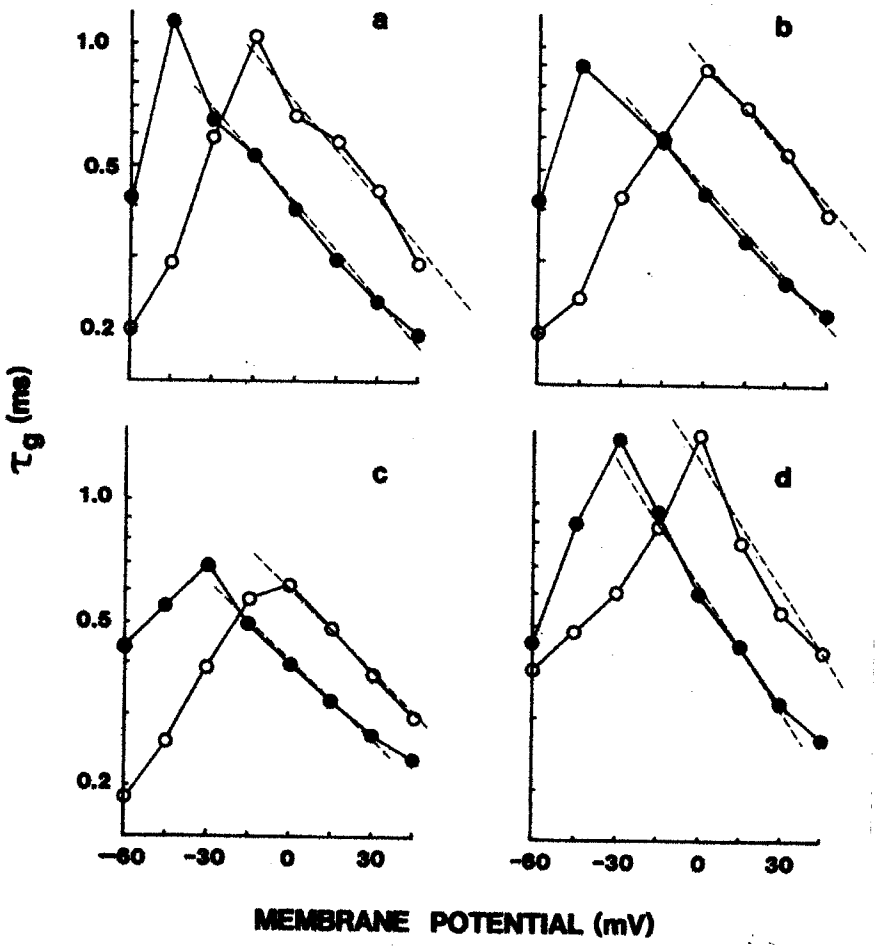

Figure 3: Gating current time constants (τ_g) at 2 (filled circles) and 40 mM Ca (open circles). τ_g is the slower of the two time constants determined by fitting the sum of two exponentials to gating currents. Estimates of the voltage shift in were made by drawing parallel lines through the points to the right of the largest time constants (illustrated by the dashed lines) and measuring the voltage of offset between the tow dashed lines. (a) Fiber 93, temperature 5°C. (b) Fiber 111, temperature 4°C. (c) Fiber 70, temperature 6°C. (d) Fiber 107, temperature 4°C. For all fibers, the holding potential was –150 mV. (From Hahin and Cambell, 1983)

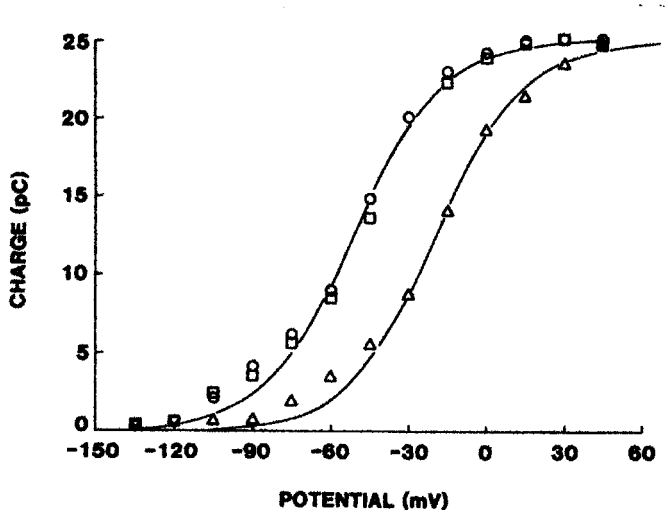

Figure 4: High Ca shifts the charge vs. voltage relationship. Points represent the gating charge obtained by integrating the gating current transients at each voltage. Circles and squares represent the before and after control curves determined in 2 mM Ca. The curve through these control points is a two-state Boltzmann distribution assuming a maximum charge of 25 pC, a valence of 1.42, and a midpoint of –51 mV. The curve through the points determined when the fiber was bathed in 40 mM Ca (triangles) is the same curve, but with a midpoint of –19 mV. Fiber 111, temperature 4° C, holding potential –150 mV. (From Hahin and Cambell, 1983)

TABLE I

Effects of a 20-fold increase in extracellular [Ca] on Na and gating currents

Activation shift	31.8 $\pm$.8 mV
h_∞ Inactivation shift	30.7 $\pm$.2 mV
τ_h Inactivation shift	32.3 $\pm$.8 mV
Q Gating current shift	30.8 $\pm$.0 mV
τ_g Gating current shift	30.7 $\pm$.6 mV

(From Hahin and Campbell, 1983)

Another example of the confirmation of Gouy-Chapman predictions is work on the potassium channel of the squid giant axon (Gilbert and Ehrenstein, 1969; Ehrenstein and Gilbert, 1973). In this case, it was possible to decrease the calcium concentration from the control value as well as to increase it. Since the squid axon preparation is ordinarily rather unstable in low calcium, the experiments were performed in high potassium solutions, where the axon is depolarized at rest and more stable in low calcium. Figs. 5 and 6 show the shifts in the conductance vs. voltage curve and in the time constant vs. voltage curve, and Table II summarizes these voltage shifts. For an increase in calcium concentration from 10 mM to 160 mM, Table II indicates a voltage shift of between 10 and 13 mV in the depolarizing direction. For an decrease in calcium concentration from 10 mM to nominal zero, Table II indicates a voltage shift of between 24 and 28 mV in the hyperpolarizing direction.

TABLE II

Voltage shifts of voltage-dependent parameters of potassium channels caused by changes in extracellular [Ca]

Calcium concentration	K conductance (g_k)	K time constant (τ_k)
0 mM	-28 mV	-24 mV
10 mM	0 mV	0 mV
160 mM	+13 mV	+10 mV

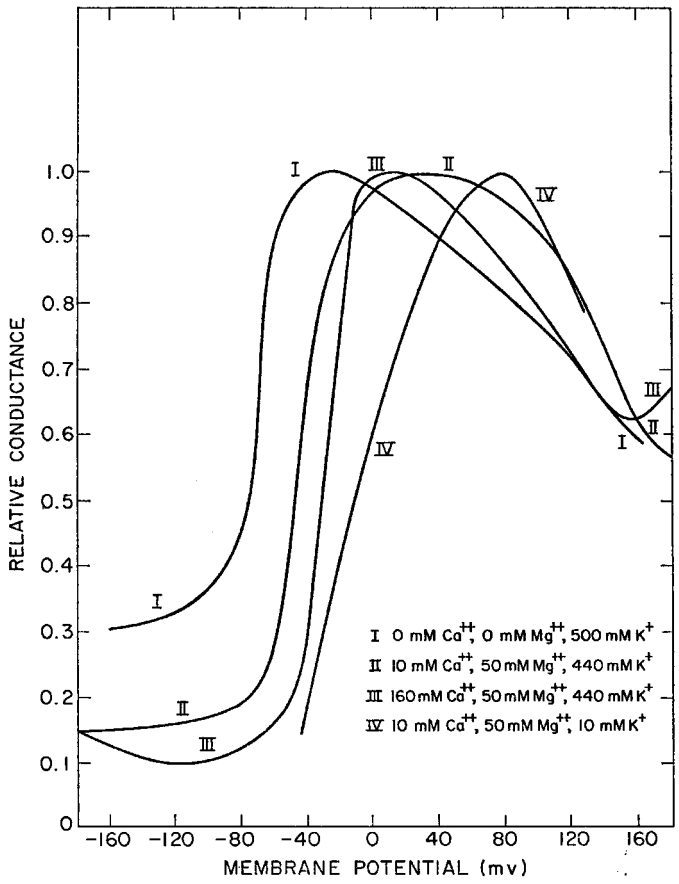

Figure 5: Steady-state conductnce vs. membrane potential. Curves I, II, III correspond to curves I, II, III in Figure 1. Curve IV is for an axon immersed in seawater. (From Gilbert and Ehrenstein, 1969)

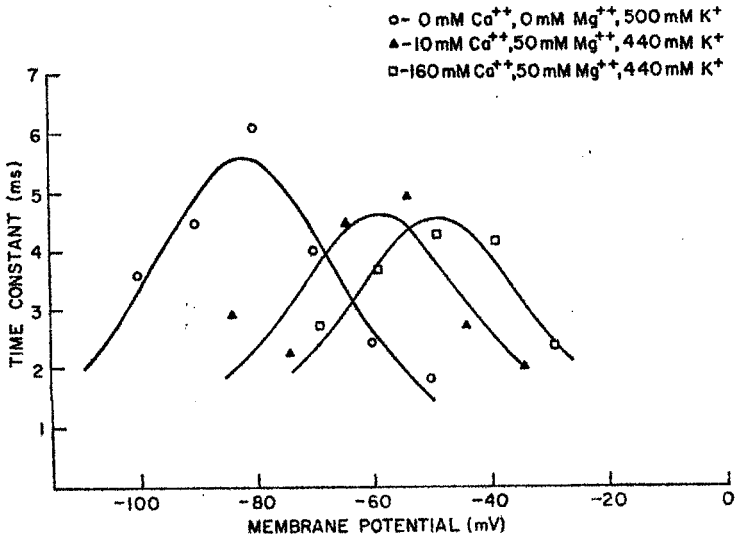

Figure 6: τ_n vs. membrane potential for various divalent cation concentrations. (From Ehrenstein and Gilbert, 1973)

There are many other measurements of voltage shifts that are consistent with the surface-charge theory. A summary of experiments where voltage shifts caused by changes in divalent ion concentration were measured for a variety of preparations and for several ion channels is shown in Table III. Values for surface charge based on Gouy-Chapman theory are also shown in Table III. The general agreement between these measurements and the Gouy-Chapman theory suggests the validity of the general view that a surface charge leads to formation of a double layer, that the double layer affects the membrane potential, and that neutralization of the surface charge reduces the effect of the double layer.

TABLE III

External surface charge for several preparations and several channels based on measurements with varying concentrations of divalent cations

Channel	Preparation	Charge Density (electron charges per nanometer^2)	Reference
K	Squid axon	0.83	Begenisich (1975) based on data of Frankenhaeuser andHodgkin (1957)
K	Squid axon	0.83	Gilbert and Ehrenstein (1969)
K	Frog node	0.17	Mozhayeva and Naumov (1970)
K	Frog node	0.34	Begenisich (1975) based on data of Brismar (1973)
K	Frog node	0.50	Vogel (1974)
K	Myxicola	0.31	Begenisich (1975)
K	Myxicola	1.3	Schauf (1975)
K	Squid axon	0.55	Fohlmeister and Adelman (1982)
Na	Squid axon	0.83	Begenisich (1975) based on data of Frankenhaeuser and Hodgkin (1957)
Na	Frog node	0.63	Begenisich (1975) based on data of Brismar (1973)
Na	Crayfish	2.3	d'Arrigo (1973)
Na	Frog node	1.4	Vogel (1974)
Na	Myxicola	0.83	Begenisich (1975)
Na	Myxicola	1.3	Schauf (1975)
Na	Tunicate egg	1.2	Ohmori and Yoshii (1977)
Na	Frog muscle	0.9	Hahin and Campbell (1983)
Ca	Tunicate egg	1.2	Ohmori and Yoshii (1977)
Ca	Snail neuron	1.3	Wilson et al. (1983)
Ca	Purkinje fiber	0.40	Kass and Krafte (1987)

An objection to the surface-charge theory is that some data do not agree with the Gouy-Chapman predictions. This will be discussed in the next Section. Another objection is that there are alternative explanations for the observed voltage shifts. For example, it has been proposed that the blocking of ion channels by divalent cations could account for the reduction of activation when

calcium is added (Stephens, 1969; Fishman et al., 1971; Moore and Jakobsson, 1971; Armstrong and Cota, 1990). This reduction of activation would appear as a depolarizing voltage shift of conductance-voltage curves. For potassium channels, this objection has been refuted by experiments performed under conditions where a voltage-dependent parameter, the time constant associated with the potassium conductance, has a clear maximum (Ehrenstein and Gilbert, 1973). Gouy-Chapman theory predicts that addition of a neutralizing divalent cation would cause the time constant versus voltage curve to shift to the right along the voltage axis, and this has been observed, as shown in Fig. 6. Such a shift corresponds to shortening of time constants to the left of the maximum and lengthening of time constants to the right of the maximum, in agreement with experiment (Ehrenstein and Gilbert, 1973). By contrast, the blocking model predicts that addition of a blocking divalent cation would always shorten the time constant. This disagreement between the blocking model and the experimental results shown in Fig. 6 does not conflict with evidence that divalent cations do block voltage-dependent channels. Rather, it indicates that any blocking by divalent cations is not the cause of the observed shifts for potassium channels.

The experimental strategy described above involves the measurement of voltage-dependent parameters. Interesting variants of this strategy focus on the effects of surface charge on ion concentration. For example, single-channel conductance is affected by the concentration of permeant ions near the channel, and this, in turn, is affected by the surface charge and the resulting surface potential. Thus, the dependence of single-channel conductance on the concentration of neutralizing divalent cations (or neutralizing impermeable monovalent cations) can be used to determine surface potential and the related surface charge. This approach was used to determine the surface charge and surface potential for inward rectifier channels in embryonic chick ventricle cells (Kell and DeFelice, 1988). Measurement of the single-channel conductance of this channel as a function of the concentration of neutralizing cations leads to a value of -40 mV for surface potential and -0.25 e/nm^2 for surface charge density. The latter value is within the range of surface charge densities shown in Table III.

An example of the determination of the effects of surface charge on carriers, rather than channels, is the measurement of the conductance of ion-carrier complexes in phospholipid membranes (McLaughlin et al., 1971). In this case, conductance is affected by the concentration of charged ion-carrier complexes, and this, in turn, is affected by the surface charge and the resulting surface potential. For negatively charged phosphotidylserine membranes, a tenfold increase in the concentration of neutralizing cations leads to a 27 mV change of surface potential. For neutral phosphotidylethanolamine membranes, by contrast, a tenfold increase in the concentration of neutralizing cations does not affect the surface potential.

IV Experimental Evidence Disagreeing with Gouy-Chapman Theory

There are some experimental results that are not consistent with Gouy-Chapman theory. A particularly clear example is the effect of zinc on both ionic currents and gating currents of the sodium channel of the squid giant axon (Gilly and Armstrong, 1982). When zinc was added to the extracellular solution, the observed shifts of voltage-dependent parameters differed considerably among the several voltage-dependent parameters. For addition of 30 mM Zn, the mean shift of the sodium conductance-voltage curve along the voltage axis was 8.4 mV, but the curve for the voltage dependence of "on" conductance kinetics was shifted by 29 mV and the curve for the voltage dependence of "off" conductance kinetics was shifted by 2 mV. There were also large differences in shifts for parameters associated with gating currents. For addition of 30 mM Zn, the mean shift of the gating charge-voltage curve along the voltage axis was 6.5 mV, but the curve for the voltage dependence of "on" gating kinetics was shifted by 27 mV and the curve for the voltage dependence of "off" gating kinetics was shifted by 6 mV. These inconsistencies with Gouy-Chapman theory are summarized in Table IV.

TABLE IV

Shifts of g_{Na} parameters and gating current parameters by 30 mM Zn

	G_{Na}	gating current
ON kinetics	+29.5 mV	+27.5 mV
OFF kinetics	+2 mV	+6 mV
g-V curve	+8.4 mV	
Q-V curve		+6.5 mV

(From Gilly and Armstrong, 1982)

Another example of experimental results that are inconsistent with Gouy-Chapman theory is the effect on sodium channels of substituting lanthanum for calcium in clonal pituitary (GH3) cells. This caused a positive voltage shift of the voltage dependence of opening rate and open-fraction curves, but a negative voltage shift of the voltage dependence of the closing rate curve (Armstrong and Cota, 1990).

V Possible Resolution of Experimental Differences

The main conflict with Gouy-Chapman theory arises from the observation that, in some cases, shifts along the voltage axis differ for several parameters related to the same channel (Cf. Table IV). This could imply one or more of the following about the sodium channel of the squid giant axon:

(1) There is no significant neutralization of surface charges by divalent cations. The observed effects are caused by another mechanism.

(2) There is significant neutralization of surface charges by divalent cations, but the simple Gouy-Chapman theory is inadequate to describe it.

(3) There is significant neutralization of surface charges by divalent cations, but there are additional effects that complicate analysis of the results.

Because there are so many measurements that are in general agreement with the Gouy-Chapman theory, (1) above seems unlikely. (2) above seems much more likely. In particular, Gouy-Chapman theory implies that the surface charge does not change when the channel changes conformation, but it is quite possible that a conformational change rearranges the channel in such a way as to change the effective surface charge. A specific model of this type has been proposed by Gilly and Armstrong (1982). (3) above also seem likely, since there is direct evidence that divalent cations can block sodium channels.

VI Significance of Surface Charge

The voltage shifts described above, which are caused by changes in the concentration of divalent cations, do not occur under normal physiological conditions. Therefore, these voltage shifts do not affect the normal functioning of ionic channels. However, the local surface charge would affect the activity of any pharmacological agent that may be applied to the extracellular solution of nerve cells. As the result of negative surface charge, the cation activity would be considerably larger at the membrane surface than in the bulk phase, and this might influence cation flux. Indeed, this type of effect has been observed with the pharmacological agent tetrodotoxin (Hille et al., 1975).

The largest and smallest estimates of surface charge summarized in Table III differ by about an order of magnitude, but surface charge measurements for a specific channel and a specific preparation have much smaller differences. The larger differences in measured surface charge are

probably caused by differences in the specific molecular structure of the several channels. A detailed comparison between surface charge measurements and actual molecular structures is not yet available. When such a comparison does become available, it should further clarify the usefulness and the limitations of Gouy-Chapman theory.

References

Armstrong, C. M. and G. Cota (1990). Modification of sodium channel gating by lanthanum. Some effects that cannot be explained by surface charge theory. J Gen Physiol **96**: 1129-40.

Begenisich, T. (1975). Magnitude and location of surface charges on Myxicola giant axons. J Gen Physiol **66**: 47-65.

Brismar, T. (1973). Effects of ionic concentration on permeability properties of nodal membrane in myelinated nerve fibres of Xenopus laevis. Potential clamp experiments. Acta Physiol Scand **87**: 474-84.

Ehrenstein, G. and D. L. Gilbert (1973). Evidence for membrane surface from measurement of potassium kinetics as a function of external divalent cation concentration. Biophys J **13**: 495-7.

Fishman, S. N., B. I. Chodorov, and M. V. Volkenstein (1971). Molecular mechanisms of membrane ionic permeability changes. Biochim Biophys Acta **225**: 1-10.

Fohlmeister, J. F. and W. J. Adelman (1982). Periaxonal surface calcium binding and distribution of charge on the faces of squid axon potassium channel molecules. J Membrane Biol **70**: 115-23.

Frankenhaeuser, B. and A. L. Hodgkin (1957). The action of calcium on the electrical properties of squid axons. J Physiol (London) **137**: 218-44.

Gilbert, D. L. and G. Ehrenstein (1969). Effect of divalent cations on potassium conductance of squid axons: determination of surface charge. Biophys J **9**: 447-63.

Gilly, W. F. and C. M. Armstrong (1982). Slowing of sodium channel opening kinetics in squid axon by extracellular zinc. J Gen Physiol **79**: 935-64.

Grahame, D. C. (1947). The electrical double layer and the theory of electrocapillarity. Chem Rev **41**: 441.

Hahin, R. and D. T. Campbell (1983). Simple shifts in the voltage dependence of sodium channel gating caused by divalent cations. J Gen Physiol **82**: 785-805.

Hille, B., J. M. Ritchie, and G. R. Strichartz (1975). The effect of surface charge on the nerve membrane on the action of tetrodotoxin and saxitoxin in frog myelinated nerve. J Physiol **250**: 34P-35P.

Kass, R. S. and D. S. Krafte (1987). Negative surface charge density near heart calcium channels. Relevance to block by dihydropyridines. J Gen Physiol **89**: 629-44.

Kell, M. J. and L. J. DeFelice (1988). Surface charge near the cardiac inward-rectifier channel measured from single-channel conductance. J Membr Biol **102**: 1-10.

McLaughlin, S. G., G. Szabo, and G. Eisenman (1971). Divalent ions and the surface potential of charged phospholipid membranes. J Gen Physiol **58**: 667-87.

Moore, L. E. and E. Jakobsson (1971). Interpretation of the sodium permeability changes of myelinated nerve in terms of linear relaxation theory. J Theor Biol **33**: 77-89.

Mozhayeva, G. N. and A. P. Naumov (1970). Effect of surface charge on the steady-state potassium conductance of nodal membrane. Nature **228**: 164-5.

Ohmori, H. and M. Yoshii (1977). Surface potential reflected in both gating and permeation mechanisms of sodium and calcium channels of the tunicate egg cell membrane. J Physiol **267**: 429-63.

Schauf, C. L. (1975). The interactions of calcium with mpyxicola giant axons and a description in terms of a simple surface charge model. J Physiol **248**: 613-24.

Stephens, W. G. (1969). Hydrogen ion and the activation of electrically excitable membranes. Nature **224**: 547-9.

Vogel, W. (1974). Calcium and lanthanum effects at the nodal membrane. Pflugers Arch **350**: 25-39.

Wilson, D. L., K. Morimoto, Y. Tsuda, and A. M. Brown (1983). Interaction between calcium ions and surface charge as it relates to calcium currents. J Membr Biol **72**: 117-30.